CSA TN: **522343**

4 June 2019

ODY / Maxcost :

IL:-
14796676
Patron:

RAPID:LOY ILLiad 197728

COPY
Sacramento State University – Library
2000 State Univ. Dr Sacramento CA 95819-6039
916 -278-6708 lib-userservices@csus.edu

NOTICE:
This material may be protected
by copyright law (Title 17 U.S. Code)

Borrower: **RAPID:LOY**
NEW: Loyola Notre Dame Library
Lending String:

Location: 4 NORTH AVAILABLE
Call #: TA 402 .E53 2001 v.1

Journal Title: Encyclopedia of materials : science and technology /

Vol.: No: Mon/Yr:

Pages:

Article Title: Auger Electron Spectroscopy
Odyssey: 206.107.43.95

Interlibrary Loan
OFFICE USE ONLY

Search Info: 1st Date: Initials:
2nd Date: Initials:

Not on Shelf ☐ Tight Binding ☐
Lacking ☐ Poor Condition ☐
Not as Cited ☐

Notes:

Pulled by:
Updated by:
Scanned by:
Delivered by:

Interlibrary Loan **41600101**
Sacramento State University Library
2000 State Univ. Dr.
SACRAMENTO CA **95819-6039**

LIBRARY MAIL
RETURN POSTAGE GUARANTEED

NEW: Loyola Notre Dame Library

whereas water atomized powders are typically irregular in shape. This morphology is attributed primarily to the presence of an oxide film on the droplet surface prior to solidification. The oxide film opposes the forces of surface tension, thereby inhibiting spheroidization.

Bibliography

Bradley D 1973 On the atomization of a liquid by high velocity gases. *J. Phys. D. Appl. Phys.* **6**, 1724–36

Champagne A, Angers R 1980 Fabrication of powders by the rotating electrode process. *Int. J. Powd. Metall. Powd. Technol.* **16**, 359–67

Dunkley J J 1998 *ASM Handbook*. ASM International, Metals Park, OH, Vol. 7, pp. 35–52

German R M 1994 *Powder Metallurgy Science*, 2nd edn. Metal Powder Industries Federation, Princeton, NJ

Grandzol R J, Tallmadge J A 1973 Water jet atomization of molten steel. *AIChE J.* **19**, 1149–58

Lavernia E J, Wu Y 1996 *Spray Atomization and Deposition*. Wiley, New York

Lawley A 1992 *Atomization: The Production of Metal Powders*. Metal Powder Industries Federation, Princeton, NJ

Tornberg C 1992 Particle size prediction in an atomization system. *Adv. Powder Metall.* **1**, 137–50

Yue A J, Dunkley J J 1994 *Atomization of Melts for Powder Production and Spray Deposition*. Oxford University Press, Oxford

A. Lawley

Auger Electron Spectroscopy

In Auger electron spectroscopy (AES), an electron beam is used to excite the electronic states of the near surface atoms of a solid. When the atoms decay from the excited electronic state, Auger electrons are emitted, carrying band structure information which makes it possible to determine the chemistry of the near surface. The combined excitation and decay processes are shown schematically in Fig. 1 for an element exhibiting a K-level transition. To perform the chemical identification the Auger electrons are energy analyzed. The emitted Auger electron has an energy associated with the band structure of the atom in the solid emitting the electron; this Auger energy, E_{KLL}, is independent of the energy of the incident electron beam. It was this independence of the incident excitation energy that led to its discovery by Auger (1925) during cloud-chamber experiments: the track lengths associated with the Auger electrons were found to be independent of incident particle energy. The Auger process can also be stimulated with photons (electron spectroscopy for chemical analysis, ESCA) or ions, but electron excitation is still the primary approach used for dedicated Auger spectrometers.

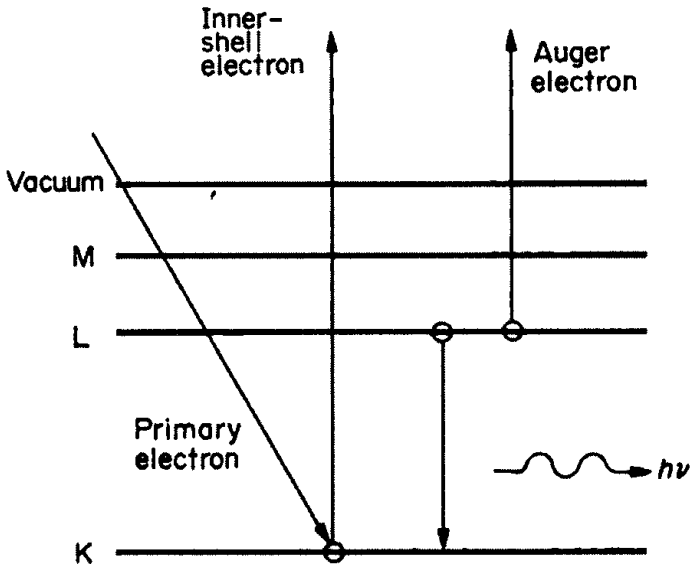

Figure 1
Schematic showing the competitive processes of x-ray and Auger electron emission. The measured energy of the emitted Auger electron is given by $E_{KLL} = E_K(Z) - E_L(Z+D) - j_A$, where Z is the atomic number, $E_K(Z)$ is the binding energy of the K-level electron, $E_L(Z)$ is the binding energy of the L-level electron, $E(Z+D)$ is the binding energy of the L-level electron in the singly ionized atom (D is a correction factor to account for the ionized state of the atom and is approximately 0.5–0.75), and j is the work function of the analyzer.

1. Probability of an Auger Decay Process

The energy released by the electron decaying from the L shell to the K shell can either be emitted as a photon (x ray) or as an Auger electron (Fig. 1). The probabilities for the two transitions are discussed by Bambynek *et al.* (1972). The most important fact is that, for the Auger electron kinetic energies of interest

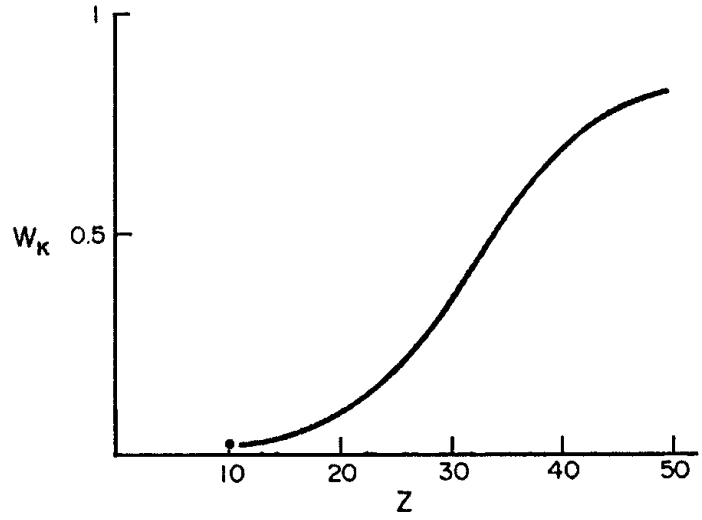

Figure 2
X-ray yield as a function of atomic number.

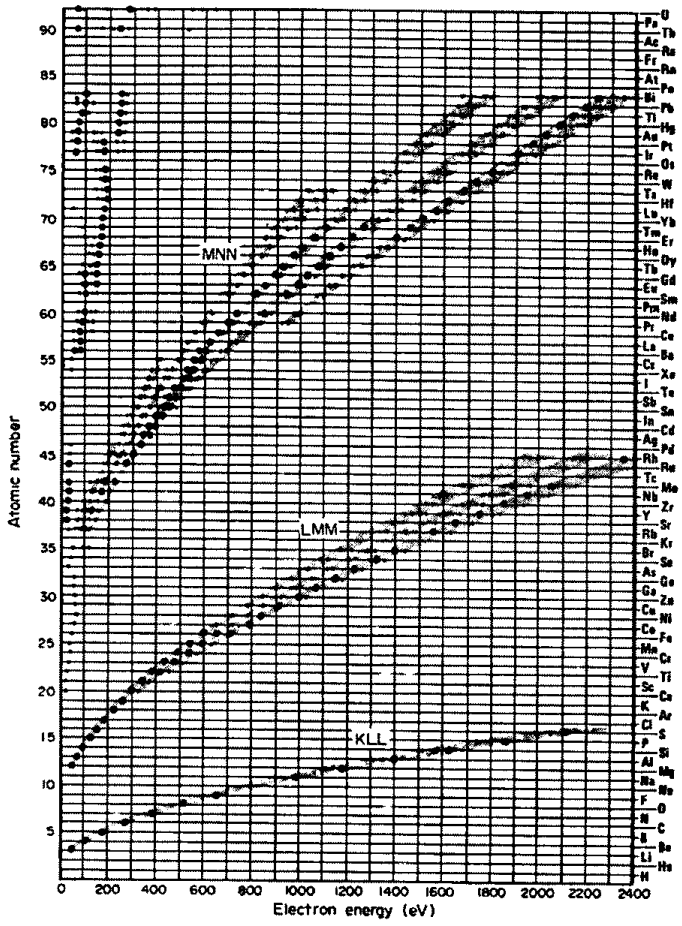

Figure 3
Characteristic Auger electron energies: dots indicate the electron energies of the principal Auger peaks for each element; large dots represent predominant peaks for each element.

in AES (0–2500eV, corresponding to atomic number $Z < 15$), as defined by the escape depth (see Sect. 2), the dominant decay process is the emission of Auger electrons. This is shown schematically in Fig. 2 for the K vacancy, where $W_K + A_K = 1$, with W_K and A_K being the probabilities of x-ray and Auger electron emissions, respectively.

When the energy of the E_{KLL} Auger electron is greater than the energy of interest for AES, the energies of the higher-level three-electron process transitions (LMM, MNN, NOO) are measured. Figure 3 shows the energy of the Auger electron as a function of atomic number. The systematic relationship between the energy and the atomic numbers within a given type of transition is readily apparent.

2. *Escape Depth*

The factor that is most important in AES, and which makes it an important experimental method for surface characterization, is the escape depth, d, of the

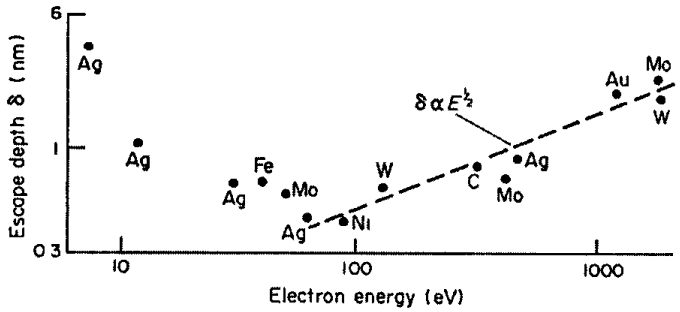

Figure 4
Escape depth d as a function of the Auger electron energy.

Auger electrons from the solid. The escape depth is the characteristic distance below the surface from which the Auger electron can reach the surface without having an inelastic interaction with the matrix. The escape depth is defined as the distance from the surface that the electron can originate at and still have a probability of $1/e$ (i.e., 0.37) of escaping without an inelastic interaction with the matrix. Figure 4 shows the escape depth as a function of the electron kinetic energy. For 20–100eV electrons, the escape depth is less than 2.0nm, falling as low as about 0.5nm in the 50–200eV energy range. The number of Auger electrons, N, that reach the surface from a depth z below the surface where N_0 electrons originate is given by $N = N_0 e^{-z/d}$. This shows that the majority of the Auger electrons originate much closer to the surface than the characteristic escape depth, and that a significant number of Auger electrons also originate below the physical escape depth. A comparison between AES and electron microprobe analysis, in which characteristic x-rays carry the band structure and chemical information, shows that the depth examined with the microprobe ($\sim$ 0.5mm characteristic x-ray electron escape depth) is about 500 times that of AES ($\sim$ 1nm). This clearly shows the advantages of AES in making measurements where local surface chemistries vary from the bulk chemistry.

3. *Auger Signal*

Many factors are involved in determining the Auger current from a given transition. For the ith transition the Auger current I_i can be represented by:

$$I_i = AI_r X_r d B j Y_i R T \qquad (1)$$

where A is the surface area irradiated; I_r is the incident current density; X_r is the concentration of element I in the irradiated volume; r is the atomic density; d is the escape depth (mean free path); B is the backscattering factor (> 1); j is the ionization cross-section; Y_i is the Auger transition probability; R is a surface roughness factor; and T is the instrument transmission. These

factors are not necessarily independent. Both j and Y_i depend on the incident electron energy, which ranges from 1 to 10keV.

4. *Ionization and Backscattering Cross-sections*

The ionization cross-section j is shown schematically in Fig. 5. The incident energy E_0 of the electron must be at least equal to the ionization energy E_w to create a hole in the w band (where w = K, L, M, N, ...). The cross-section increases up to an incident electron energy of about three times the ionization energy, and slowly falls off after about six to eight times the ionization energy. The relatively slow falloff in cross-section with increasing incident energy is due to the influence of the backscattered electrons creating additional electron holes in the w band. These electrons also influence the spatial resolution of the electron beam, since they diverge as they exit the specimen. This enlarges the region of surface that is analyzed. In addition, the backscattering factor B will vary with the substrate: high-Z elements will backscatter a larger fraction of the incident electrons. This leads to modification of the signal intensity in thin-layered structures.

5. *Auger Peak Widths*

The Heisenberg uncertainty principle can be expressed as $DEDt \geqslant h/2p$, where h is Planck's constant ($\sim 4 \times 10^{-15}$eVs) and $Dt@t_{1/2}$ ($\sim 10^{-16}$s) is the half-life of the initial ionization state. Therefore, $DE \geqslant h/2pDt \sim$ 6eV, which is approximately the natural Auger line width, G. Additional line broadening results from the width of the outer or valence bands, from complicated band structure, and from instrumental broadening which occurs because of the convolution of the instrument function and the natural line shape.

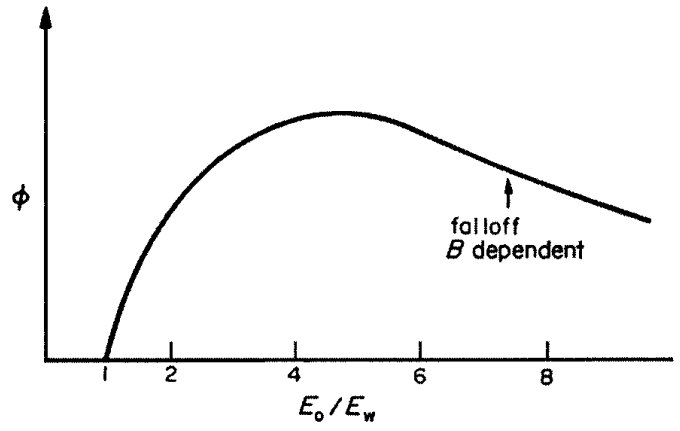

Figure 5
Schematic of ionization cross-section (arbitrary units) as a function of the ratio of the primary energy to the ionization energy.

When $DE_{instrument} \geqslant G$, instrumental broadening occurs, but when $DE_{instrument}$ is significantly less than G, the effect on peak width by the instrument is small.

6. *Measurement of Auger Electron Energy*

There are several methods used to energy analyze the Auger electron. They include: (i) a retarding-grid system, often used in conjunction with low-energy electron diffraction (LEED); and (ii) velocity analyz-

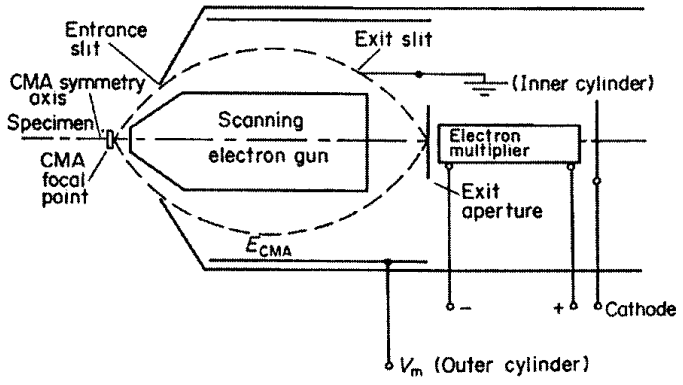

Figure 6
Schematic of a cylindrical mirror analyzer.

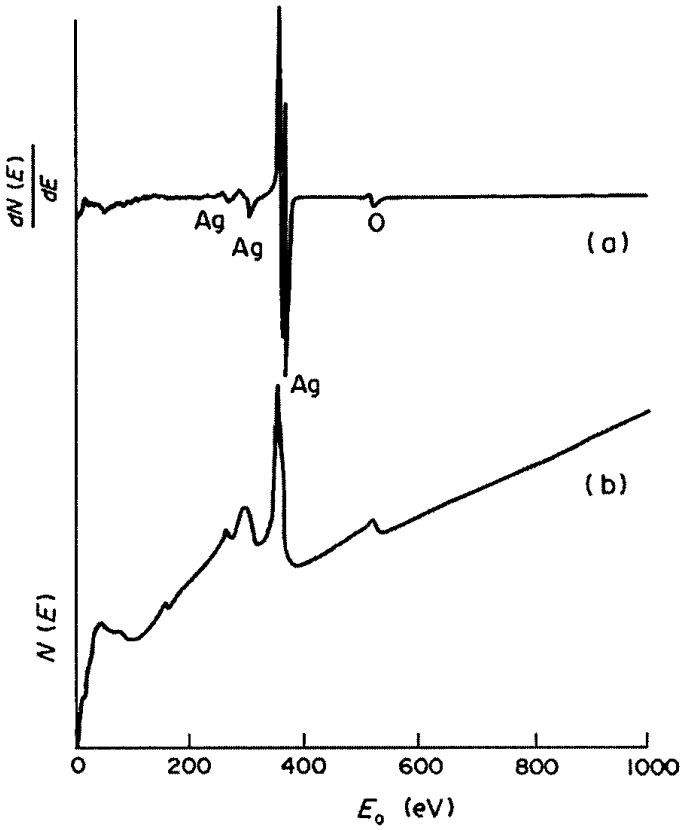

Figure 7
AES spectrum of silver: (a) derivative mode; (b) energy distribution mode.

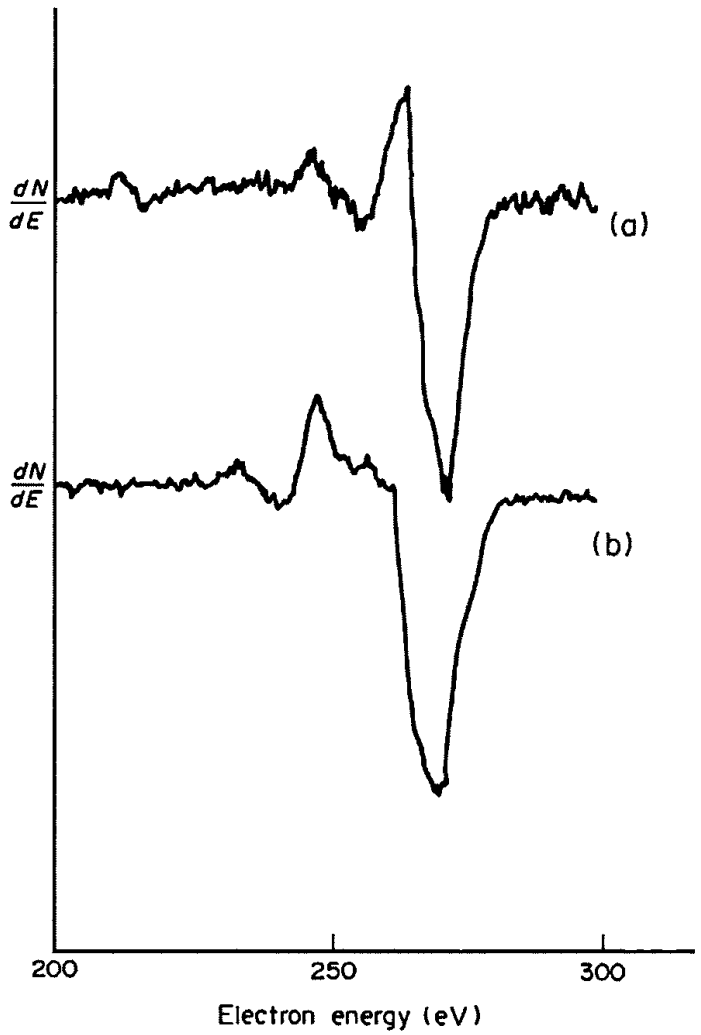

Figure 8
Characteristic carbon peaks for (a) carbide and (b) graphite.

ers, which include 270° sectors, cylindrical mirror analyzers (CMAs), and spherical analyzers. The CMA is the most commonly used electron energy analyzer. Figure 6 is a schematic of a CMA, showing the orientation of the sample relative to the analyzer and the scanning electron gun coaxial with the CMA. The focused scanning electron beam leads to a useful spatial resolution of AES of less then 50 nm using a field emission electron gun. This allows detailed local spatial chemical analysis of the surface. The voltage V_m applied to the outer cylinder selectively bends the electrons to be counted on the electron multiplier. Ramping the voltage sweeps the electron energy analyzed across the energies of interest in AES. The current measurement is directly proportional to the electron energy distribution $N(E)$. Superimposing a high-frequency low-amplitude signal on the ramping voltage, and electronically locking in on that frequency to select that Fourier component of the analyzed electron signal, gives a current that is related to $dN(E)/dE$. This technique, developed by Harris (1968), strongly enhances the signal-to-noise ratio of the Auger spectrum. $N(E)$ and the corresponding $dN(E)/dE$ are shown in Fig. 7 for the MNN AES peaks of silver. Most current AES instruments directly measure $N(E)$ and differentiate it using appropriate computer software.

7. *Chemical Effects in AES*

The integrated Auger peaks give direct information about how much of each element is present in the volume analyzed. In addition, the Auger peaks' shapes and locations carry information about the chemical state of the atoms (see *Chemical Analysis, Electron Spectroscopy*). Figure 8 shows the $dN(E)/dE$ peak shapes for carbon, in a graphitic form and in Al_4C_3. Similar peak shape changes are seen for oxides, sulfides, borides and many other bonding states of the atoms. Standards are used to define the peak shapes kinetic energy of the peaks.

8. *Quantitative Auger Analysis*

The simplest form of quantitative AES uses the differentiated peak heights for elemental standards under the same operating conditions; this gives a reasonable measure of each element present. Another method is to use standards of the approximate chemistry expected; the difficulty is in preparing a standard surface chemistry, even if the bulk chemistry is defined. Integration of the $N(E)$ can also be used for quantitative analysis. Other problems in quantitative AES are related to the presence of thin variable-chemistry layered structures, and the interaction between layers as related to the origin of the Auger signal described in Sect. 3.

9. *AES Depth Profiling*

Much of the information of interest in AES studies is not only at the surface, but is present also in thin-layered regions in the near-surface region. To make it possible to analyze these near-surface regions, Marcus and Palmberg (1969) combined inert-ion sputtering with AES. This enabled the chemical profiles normal to the surface of interest to be determined, and is standard practice in AES. Combined AES and inert-ion sputtering has been used to show the localized nature of surface and interface equilibrium segregation, as well as to analyze more diffuse chemical distributions. The experimental approach is to bombard the surface with an ionized gas, usually argon, in the kinetic energy range 500–5000 eV. The sputtered surface is continuously or "intermittently" analyzed with AES. In some systems, secondary-ion mass

spectroscopy (SIMS) may be carried out simultaneously with the AES analysis to give complementary information.

Ion sputtering can introduce artifacts into the surface region, and the potential for such artifacts must be carefully considered in any measurement. Preferential sputtering of one atom species over another, in particular at low ion voltage, occurs very often, producing artificial chemical profiles. The ion beam also may do structural damage to the surface, changing the local chemical bonding. For example, carbides from free graphite have been formed under the influence of the inert-ion beam (see *Depth Profiling*)

Another major problem with inert-ion sputtering is the very difficult task of quantifying the depth sputtered. Standard sputtering rates for homogeneous materials can be measured, but may not be directly related to sputtering of sequential thin-layer structures of varying chemistry. Here again, the difficulty of preparing thin-layered standards limits the ability to determine the sputtering depth. To overcome edge effects associated with the ion-beam shape, the ion beam is rastered and AES is performed only in the middle where a relatively uniformly sputtered area exists.

10. Vacuum Requirements for AES

The extreme surface sensitivity of AES makes it a mandatory requirement that, in order to get good information, the surface must be kept clean. This is particularly true for the case of very thin layers of material. For this reason, AES must be done in a vacuum system with a very low partial pressure of active gases, in particular H_2O. To have minimal interference with the electron optics, a vacuum of better than 10^{-2} Pa is required. If the primary constituents of the vacuum are inert gases and the partial pressure of the active gases in the chamber is below 10^{-7} Pa, then clean surfaces can be maintained during the measurement time. It should be noted that an active gas with a sticking coefficient of unity will cover the surface with a monolayer for $\sim$ 1 s exposure at 10^{-4} Pa.

Therefore, there is a need for high vacuum with minimal active gases. To obtain this, all-metal systems are preferred. In certain cases, limited amounts of low-vapor-pressure nonmetallic O-ring seals can be used. Good vacuum practice must be followed to avoid virtual leaks in the system. For most systems a transfer chamber is used to introduce samples. This limits the volume of the chamber that is exposed to the external environment, thereby reducing contamination and maintaining low pressures in the chamber.

To obtain the vacuum, most systems avoid oil pumping systems but use a combination of zeolite-sorption pumps to rough pump the system, and ion pumps combined with titanium sublimation pumps to obtain the best ultimate pressure. Where quick turnaround time is required, heavily trapped turbomolecular pumps are used.

It should be noted that the nature of the surface will have a significant influence on how good a vacuum is required. For semiconductor and oxide materials the requirements are much less stringent than for clean surface-active metals, such as aluminum, titanium and iron. For the surface-active materials, it is advisable to prebake the system at about 200 °C to desorb the water vapor from the walls of the chamber. The baking greatly reduces the relative partial pressure of water vapor present and lowers the absolute pressure of the system to the low 10^{-8} Pa range.

11. Application of AES

The use of AES is very widespread across the scientific and engineering disciplines. Many of the major uses of materials are controlled by surface or interface properties, as well as by thin-layered structures. In metal-

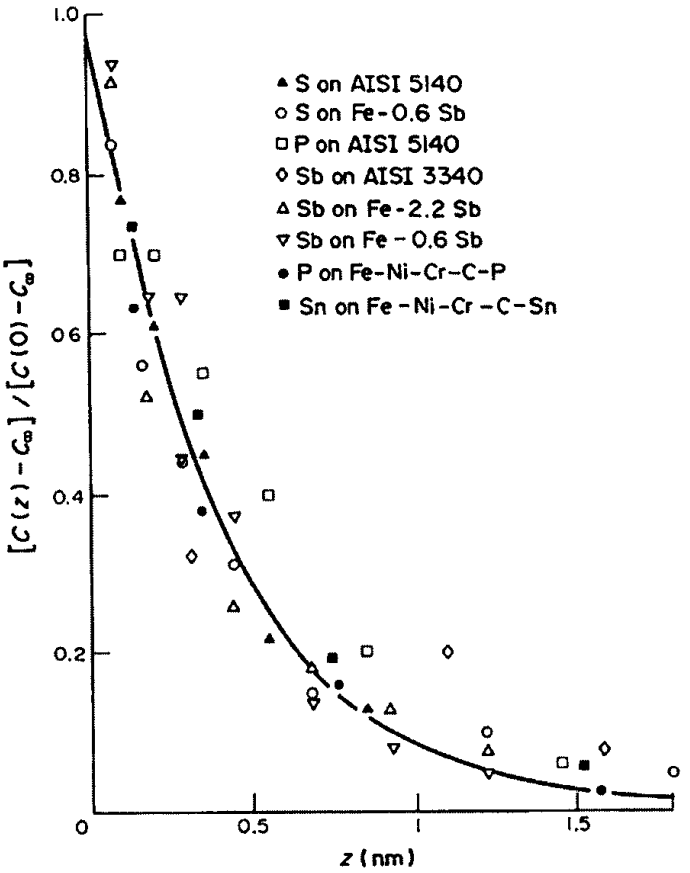

Figure 9
Sputter profile from intergranular fracture surfaces of steel: $C(z)$ is the concentration of the element at a depth z below the surface; $C(0)$ is the concentration at the surface; C is the concentration in the bulk material.

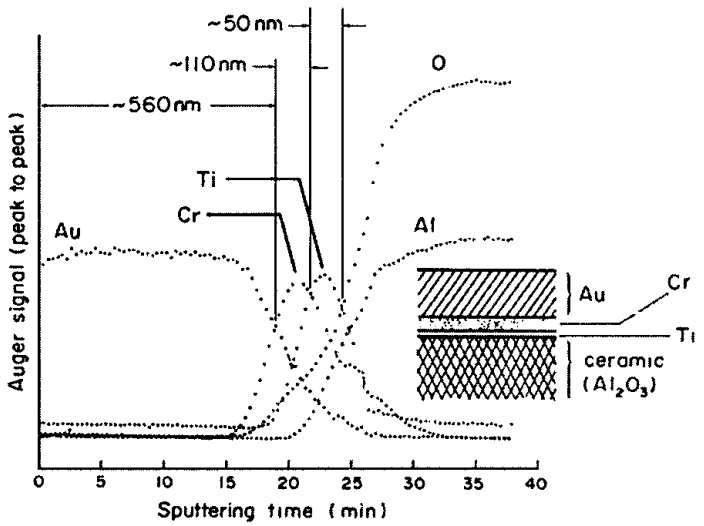

Figure 10
Sputter profile through a semiconductor layered structure.

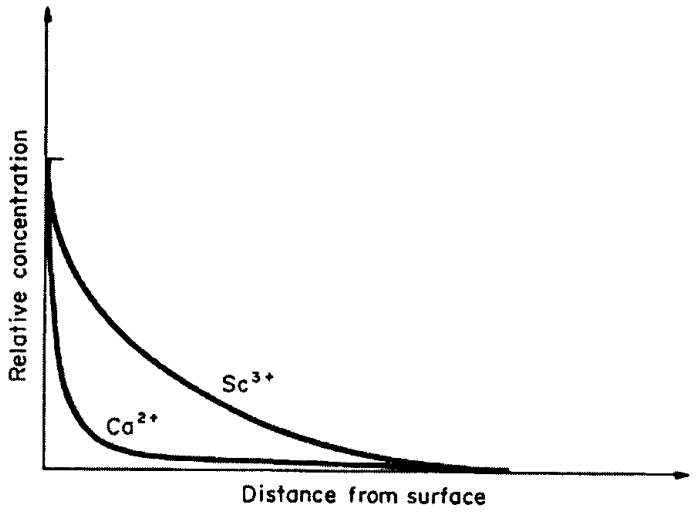

Figure 11
Sputter profile of segregation to free surface of Ca^{2+} and Sc^{3+} in MgO.

lurgy, the areas of fracture and fatigue, where new surfaces are created, bulk and grain boundary diffusion, coatings, adhesion, surface preparations, hydrogen embrittlement, solidification, powder metallurgy, composites, diffusion bonding, and others all have problems related to surfaces and interfaces, and have gained insights from AES studies. A prominent example has been the extensive studies on grain-boundary and interface fracture in steels; Fig. 9 is an inert-ion sputtering profile showing the local nature of grain-boundary segregation associated with equilibrium segregation.

Similar types of results are obtained in semiconductor studies. The thin-layered structures of high-device-density electronic materials lead to the requirement of AES as a quality control system. Localized elements that influence the electrical properties of the materials can be identified using the surface-sensitive AES. An example of a semiconductor layered structure is given in Fig. 10.

Another area where AES acts as a dynamic probe is the study of the catalytic behavior of materials. In this case, most of the catalytic properties are established by the surface chemistry and bonding. AES chemical and bonding information has proved extremely valuable in obtaining understanding of catalytic behavior and in leading the way to improve the catalysts. Other areas in which AES has been applied are lubrication, friction and wear, and the general area of tribology. AES has identified the transfer and residual films associated with these processes.

Ceramics have also been studied in some detail. Both interface chemistry and its relation to densification, as well as surface segregation, have been evaluated. Figure 11 shows a depth profile from a surface of MgO. The profiles show that the segregated Ca^{2+} ions are very near the surface, but Sc^{3+} ions are more diffusely distributed because of the need for charge neutrality in the bulk.

See also: Chemical Analysis, Electron Spectroscopy; Depth Profiling

Bibliography

Auger P 1925 Sur l'effet photoelectrique compose. *J. Phys. Radium* **6**, 205–6

Bambynek W, Crasemann B, Fink R W, Freund H-U, Mark H, Swift C D, Price R E, Rao V P 1972 X-ray fluorescence yields, Auger, and Coster-Kronig transition probabilities. *Rev. Mod. Phys.* **44**, 716–813

Harris L A 1968 Analysis of materials by electron excited Auger electrons. *J. Appl. Phys.* **39**, 1419–27

Marcus H L, Palmberg P W 1969 Auger fracture surface analysis of a temper embrittled 3340 steel. *Trans. Metall. Soc. AIME* **245**, 1664–6

H. L. Marcus

Austenite at Room and Low Temperature, Deformation and Fracture of

Austenitic steels are Fe-based alloys that are highly alloyed to stabilize the f.c.c. structure at room temperature and below. The commonest austenite stabilizers are the substitutional species, nickel and